Pergamon

Geochimica et Cosmochimica Acta, Vol. 68, No. 5, pp. 1049–1059, 2004

0016-7037/04 $30.00 + .00

doi:10.1016/S0016-7037(03)00371-5

Thermodynamics of iron oxides: Part III. Enthalpies of formation and stability of ferrihydrite (~$Fe(OH)_3$), schwertmannite (~$FeO(OH)_{3/4}(SO_4)_{1/8}$), and ε-Fe_2O_3

J. MAJZLAN,[1,2,*] A. NAVROTSKY,[1] and U. SCHWERTMANN[3]

[1]Thermochemistry Facility and Department of Geology, University of California at Davis, Davis, CA 95616, USA
[2]Department of Geosciences, Princeton University, Princeton NJ 08544, USA
[3]Technische Universität München, Lehrstuhl für Bodenkunde, D-85350 Freising-Weihenstephan, Germany

(*Received January* 13, 2003; *accepted in revised form May* 15, 2003)

Abstract—Enthalpies of formation of ferrihydrite and schwertmannite were measured by acid solution calorimetry in 5 N HCl at 298 K. The published thermodynamic data for these two phases and ε-Fe_2O_3 were evaluated, and the best thermodynamic data for the studied compounds were selected.

Ferrihydrite is metastable in enthalpy with respect to $\frac{1}{2}$ α-Fe_2O_3 and liquid water by 11.5 to 14.7 kJ•mol^{-1} at 298.15 K. The less positive enthalpy corresponds to 6-line ferrihydrite, and the higher one, indicating lesser stability, to 2-line ferrihydrite. In other words, ferrihydrite samples become more stable with increasing crystallinity. The best thermodynamic data set for ferrihydrite of composition $Fe(OH)_3$ was selected by using the measured enthalpies and (1) requiring ferrihydrite to be metastable with respect to fine-grained lepidocrocite; (2) requiring ferrihydrite to have entropy higher than the entropy of hypothetical, well-crystalline $Fe(OH)_3$; and (3) considering published estimates of solubility products of ferrihydrite. The ΔG^o_f for 2-line ferrihydrite is best described by a range of -708.5 ± 2.0 to -705.2 ± 2.0 kJ•mol^{-1}, and ΔG^o_f for 6-line ferrihydrite by -711.0 ± 2.0 to -708.5 ± 2.0 kJ•mol^{-1}.

A published enthalpy measurement by acid calorimetry of ε-Fe_2O_3 was re-evaluated, arriving at ΔH^o_f (ε-Fe_2O_3) = -798.0 ± 6.6 kJ•mol^{-1}. The standard entropy (S^o) of ε-Fe_2O_3 was considered to be equal to S^o (γ-Fe_2O_3) (93.0±0.2 J•K^{-1}•mol^{-1}), giving ΔG^o_f (ε-Fe_2O_3) = -717.8 ± 6.6 kJ•mol^{-1}. ε-Fe_2O_3 thus appears to have no stability field, and it is metastable with respect to most phases in the Fe_2O_3-H_2O system which is probably the reason why this phase is rare in nature.

Enthalpies of formation of two schwertmannite samples are: ΔH^o_f ($FeO(OH)_{0.686}(SO_4)_{0.157}$•$0.972H_2O$) = -884.0 ± 1.3 kJ•mol^{-1}, ΔH^o_f ($FeO(OH)_{0.664}(SO_4)_{0.168}$•$1.226H_2O$) = -960.7 ± 1.2 kJ•mol^{-1}. When combined with an entropy estimate, these data give Gibbs free energies of formation of -761.3 ± 1.3 and -823.3 ± 1.2 kJ•mol^{-1} for the two samples, respectively. These ΔG^o_f values imply that schwertmannite is thermodynamically favored over ferrihydrite over a wide range of pH (2–8) when the system contains even small concentration of sulfate. The stability relations of the two investigated samples can be replicated by schwertmannite of the "ideal" composition $FeO(OH)_{3/4}(SO_4)_{1/8}$ with ΔG^o_f = -518.0 ± 2.0 kJ•mol^{-1}. *Copyright © 2004 Elsevier Science Ltd*

1. INTRODUCTION

Iron oxides in natural settings are represented by a variety of minerals that range from well to poorly crystalline. Examples of the former include hematite and goethite, and the latter include ferrihydrite (2-line, 6-line), schwertmannite, feroxyhyte, and "green rust." The poorly crystalline iron oxides act as precursors to the well-crystallized ones. Because of their high surface area and reactivity, the poorly crystalline minerals are active in many processes, such as adsorption and transport of metals from acid mine drainage waters (Jambor and Dutrizac, 1998). Ferrihydrite, a material of ambiguous identity, was used in a number of laboratory studies on adsorption and transport of metals, pesticides, herbicides, and organic nutrients in the environment (Clausen and Fabricius, 2001; Scheinost et al., 2001; Leone et al., 2002). The question of the structure of ferrihydrite was addressed by Janney et al. (2000a, 2000b, 2001), Drits et al. (1993), Manceau and Drits (1993), and Jansen et al. (2002). ε-Fe_2O_3 is not known as a mineral but has been reported as a constituent of iron oxide clusters in living organisms (McClean et al., 2001). Its crystal structure was studied by Tronc et al. (1998). In a first approximation, schwertmannite can be considered as a disordered akaganeite-like phase, with the tunnels occupied by sulfate instead of chloride (Bigham et al., 1990). Waychunas et al. (2001) found the sulfate anions as inner and outer sphere complexes on the surfaces of schwertmannite crystallites, rather than in the tunnels.

The thermodynamics of the well-crystalline iron oxides (hematite, goethite, lepidocrocite, maghemite) has been a subject of numerous studies (see Majzlan et al., 2003b), which suggest that hematite and goethite define the energetic and thermodynamic minimum of the system Fe_2O_3-H_2O. Laberty and Navrotsky (1998) investigated thermochemistry of akaganeite and found hypothetical β-FeOOH to be slightly metastable with respect to goethite. Some thermodynamic data on the poorly crystalline iron oxides are available in the literature (Bigham et al., 1990; Yu et al., 1999; Kawano and Tomita, 2001); however, they mostly represent estimates based on solubility studies of somewhat ill-defined natural samples. The disagreement among the published values stems from extreme variability of the natural poorly crystalline iron oxides in terms of chemical composition and structure.

* Author to whom correspondence should be addressed (jmajzlan@princeton.edu).

In this study, we limited our attention solely to poorly crystalline iron oxides. We measured enthalpies of formation of ferrihydrite and schwertmannite by acid solution calorimetry, and re-evaluated the available data on thermochemistry of synthetic ε-Fe_2O_3. ε-Fe_2O_3 was included despite its rare occurrence because, as one of the poorly crystalline iron oxides, it helps to create a general picture about the energetic and thermodynamic relations among the phases in the system Fe_2O_3-H_2O. The objective of this study was to constrain the thermodynamic properties of the poorly crystalline iron oxides by using well-characterized synthetic samples for direct thermochemical measurements. Natural samples were purposely avoided to reduce the number of compositional and structural variables. Though the variability of natural samples must be acknowledged, the chemical homogeneity of our synthetic samples offers a good starting point for exploration of thermodynamic properties of these difficult materials. Some of the samples used in this study were extensively characterized (e.g., Bigham et al., 1990; Janney et al., 2000a), and we augmented these samples by others, prepared specifically for this study. We then proceeded to discriminate among the published solubility products for these compounds to select the ones that best represent their thermodynamic properties and are consistent with our thermochemical measurements.

2. MATERIAL AND METHODS

2.1. Sample Synthesis

The ferrihydrite sample fh0 was prepared by rapid neutralization of ferric nitrate solution by NaOH solution (see Schwertmann and Cornell, 2000), then repeatedly washed, centrifuged and freeze-dried. The structure of this sample was investigated in detail by electron nanodiffraction (Janney et al., 2000a). A series of ferrihydrite samples (fh2, fh6, fh12, fh24) was synthesized by titrating 50 mL of 0.1 mol/L $Fe(NO_3)_3$ solution by NaOH solution of variable molarity. The rate of titration was kept constant at 1 mL of solution per minute, using a peristaltic pump. The alkaline solution was prepared and stored in a teflon beaker opened to the atmosphere, and pumped into the ferric nitrate solution via teflon tubing. Teflon was used to avoid Si contamination from glass beakers. The molarity of the alkaline solution was varied to vary titration time from 2 to 24 h. 0.6 g NaOH was dissolved in 120, 360, 720, and 1440 mL of deionized water. Each $Fe(NO_3)_3$ solution was titrated with vigorous stirring to pH = 7. Ferrihydrite was separated from the suspension by multiple centrifugation and dried at 310 K. The samples used in this study were then designated fh0, fh2, fh6, fh12, and fh24, according to the titration time in hours.

Two schwertmannite samples (B1000S, Sch18) were prepared according to the procedure described in Schwertmann and Cornell (2000). The sample B1000S was characterized by Bigham et al. (1990) in one of the early studies on schwertmannite.

The enthalpies of formation were determined with respect to lepidocrocite (γ-FeOOH), periclase (MgO), and α-$MgSO_4$. Lepidocrocite was synthesized and characterized by Majzlan et al. (2003a, 2003b) who also measured its enthalpy of formation. Periclase (Alfa Aesar, 99.99% metals basis) was heated at 1773 K overnight in a platinum crucible. Before calorimetry, the sample was kept at 1200 K in a Pt crucible in a muffle furnace. The sample was withdrawn from the furnace for each experiment; the required amount to be used in calorimetry was removed, and the sample was returned to the furnace. This procedure minimized any H_2O or CO_2 uptake of the MgO. The low-temperature modification of magnesium sulfate (α-$MgSO_4$) was synthesized by grinding 2 g of $MgSO_4 \cdot nH_2O$ ($n \sim 7$, Alfa Aesar, reagent grade) and heating the powder at 423 K in a platinum crucible for 2 h. The crucible was then withdrawn from the furnace; the product was quickly disintegrated and mixed thoroughly with 0.5 mL of concentrated sulfuric acid (96 wt.% H_2SO_4). The furnace was set at 588 K and the mixture was heated for 24 h (Ko and Daut, 1980). The mixing with sulfuric acid and 24 h heating at 588 K was repeated once. The sample was then quickly transferred, allowed to cool, and subsequently handled in a glove box with argon atmosphere (<1 ppm H_2O).

X-ray diffraction (XRD) patterns were collected using a Scintag PAD V diffractometer with Cu Kα radiation and a diffracted beam graphite monochromator. The XRD pattern of α-$MgSO_4$ was taken in an argon-filled chamber in an Inel XRG 3000 diffractometer.

2.2. Characterization Methods and Calorimetry

Before the collection of XRD patterns, chemical analyses, and calorimetric experiments, the samples were allowed to equilibrate in a controlled environment (292±2 K, 50±5% relative humidity) to ensure that the chemical composition and physical properties determined by the analyses apply precisely to the samples introduced into the calorimeter. Afterwards, the water content of the samples was determined from the weight loss upon firing overnight at 1200 K in corundum crucibles. The schwertmannite samples were analyzed for the Fe and S content by a combination of ICP-AAS techniques (Galbraith Laboratories, Inc.).

The enthalpies of solution were measured in a commercial Hart Scientific IMC-4400 isothermal calorimeter. The solvent was HCl (5 N standardized solution, Alfa Aesar) and the experiments were performed at 298 K. Calibration of the calorimeter was performed by dissolving KCl (NIST standard reference material (SRM) 1655) in deionized water. The enthalpy on the NIST certificate for SRM 1655 certificate could not be used because it refers to a specific high final KCl molality (0.111 mol/L) which could not be achieved in our experiments. Therefore, we calculated the dissolution enthalpy of KCl for molality achieved in our experiments from Parker (1965), because the compilation of Parker (1965) served as a basis for the NIST certificate and included enthalpy data for a range of final KCl molalities. The average weight of lepidocrocite pellets was 9.87±0.07(2σ) mg. All other samples were weighed out to stoichiometry with this weight.

2.3. Error Analysis

Every experimental datum that was determined in this study is associated with an uncertainty which represent two standard deviations of the mean. To calculate formation enthalpies via thermochemical cycles, the experimental data are combined and the uncertainty on the resulting value are derived by a rigorous error propagation (following Taylor 1982, p.73). The Gibbs free energy of formation (ΔG^o_f) for the studied phases was calculated from measured formation enthalpies and estimated entropies. If the entropy estimate is based on an experimentally derived value for another iron oxide (such as for ε-Fe_2O_3), the experimental uncertainty is available and the error on ΔG^o_f was calculated by error propagation. In other cases was entropy estimated from considering entropy changes for selected reactions, entropy-volume relationships, etc., and the uncertainty is unknown. In these cases, we calculate the error on ΔG^o_f considering the error on entropy to be zero. We neglect the error on entropy not only because it is difficult to estimate the uncertainty of an estimate but also because the errors on entropy contribute little to the overall error on ΔG^o_f. For example, the ΔH^o_f and S^o for maghemite are -808.1 ± 2.0 kJ•mol^{-1} and 93.0 ± 0.2 J•mol^{-1}•K^{-1}, respectively (Majzlan et al., 2003a, 2003b). The ΔG^o_f for maghemite is -727.9 ± 2.0 kJ•mol^{-1}, where the ΔH^o_f error contributed more than 99% to the ΔG^o_f error. Although the estimated entropy are certainly less precise than the values measured by adiabatic calorimetry (such as the S^o of maghemite, Majzlan et al., 2003a), we consider the errors on ΔG^o_f being dominated by errors on ΔH^o_f.

For values derived by linear extrapolation, the uncertainties were calculated by error propagation (following Taylor 1982, p. 73) with an assumption that the distribution of errors on enthalpy measurements is normal (gaussian) and that the errors on the variables plotted on abscissa and ordinate are mutually independent.

3. RESULTS AND DISCUSSION

3.1. ε-Fe_2O_3

The enthalpy of formation of ε-Fe_2O_3 was determined relative to α-Fe_2O_3 by solution calorimetry in HCl by Trautmann

Table 1. Selected thermodynamic data for the studied phases. Additional thermodynamic values used for calculating log $K_{1,8,21}$ are $\Delta G^{\circ}_f(Fe^{3+}) = -16.7 \pm 2.0$ kJ · mol^{-1}, $\Delta G^{\circ}_f(H_2O) = -237.1 \pm 0.1$ kJ · mol^{-1} (both Robie and Hemingway 1995), and $\Delta G^{\circ}_f(SO_4^{2-}) = -744.0 \pm 0.4$ kJ · mol^{-1} (Nordstrom and Munoz 1994).

	ΔG°_f (kJ · mol^{-1})	ΔH°_f (kJ · mol^{-1})	S° (J · K^{-1} · mol^{-1})	log K
ε-Fe_2O_3	-717.8 ± 6.6	-798.0 ± 6.6	93.0 ± 0.2	log $K_1 = 4.7 \pm 1.3$
2-line ferrihydrite	-708.5 ± 2.0	-827.1 ± 2.0	122.2 − 133.0	log $K_8 = 3.4 \pm 0.5$
$Fe(OH)_3$	-705.2 ± 2.0			-4.0 ± 0.5
6-line ferrihydrite	-711.0 ± 2.0	-830.3 ± 2.0	122.2 − 130.7	log $K_8 = 3.0 \pm 0.5$
$Fe(OH)_3$	-708.5 ± 2.0			-3.4 ± 0.5
Schwertmannite	-518.0 ± 2.0			log $K_{21} = 1.2 \pm 0.5$
$FeO(OH)_{3/4}(SO_4)_{1/8}$				

(1966). The difference in solution enthalpies of α- and ε-Fe_2O_3 is 28.2 ± 6.5 kJ•mol^{-1}, and combined with the currently used $\Delta H^{\circ}_f(\alpha\text{-}Fe_2O_3)$ (-826.2 ± 1.3 kJ•mol^{-1}, Robie and Hemingway, 1995), the $\Delta H^{\circ}_f(\varepsilon\text{-}Fe_2O_3)$ is -798.0 ± 6.6 kJ•mol^{-1}. Trautmann (1966) also determined the enthalpy difference between α and γ-Fe_2O_3 as 19.5 ± 6.5 kJ•mol^{-1}, in good agreement with 18.1 ± 2.4 kJ•mol^{-1} of our recent study (Majzlan et al., 2003b). As a first approximation, we assumed that the entropies of the two metastable Fe_2O_3 polymorphs (γ and ε) are equal, taking the standard entropy of γ-Fe_2O_3 from Majzlan et al. (2003a). The selected thermodynamic values for ε-Fe_2O_3 are listed in Table 1. The log K value (Table 1) was calculated for the reaction

$$\varepsilon\text{-}Fe_2O_3 + 6H^+ = 2Fe^{3+} + 3H_2O \quad (1)$$

ε-Fe_2O_3 is comparable in enthalpy to ferrihydrite, and in Gibbs free energy slightly stable with respect to ferrihydrite and liquid water but metastable with respect to all other phases in the system (Fig. 1).

3.2. Ferrihydrite

Compositions and enthalpies of solution (ΔH_{sol}) of ferrihydrite samples are listed in Tables 2 and 3, respectively. Sample fh0 was previously investigated in detail by Janney et al. (2000a) who found that this sample consists of a mixture of particles with variable structures. A significant proportion of the particles was highly disordered; others showed a continuous range between the disordered state and ordered arrays of iron coordination polyhedra. The structures distinguished in these particles are based on hexagonal and cubic close packing of anions, and are reminiscent of a double-chain and maghemite-like arrangement. For the other samples used in this study (fh2 through fh24), only bulk structural information is provided by the X-ray diffraction patterns (Fig. 2) which show increasing crystallinity in the sample series. The samples fh0 and fh2 are 2-line ferrihydrite. The samples fh6 and fh12 show five broad XRD peaks, three of those not well resolved in fh6. The sample fh24 is a 6-line ferrihydrite (Fig. 2). The ΔH_{sol} values were converted to enthalpies of formation from the elements (ΔH°_f) (Table 4) via a thermochemical cycle (Table 5). All reported enthalpies (ΔH_{sol}, ΔH°_f) are calculated per one mole of FeOOH in the formula, plus the excess water as measured, thus FeOOH•xH_2O. With increasing crystallinity, the ferrihydrite samples become more stable. The difference in ΔH_{sol} between 2-line and 6-line ferrihydrite is appreciable (3.2 ± 0.6 kJ•mol^{-1}) but in terms of the enthalpies of formation from elements, the enthalpy values for the individual samples are significantly further apart (Table 4). This is caused by variable amount of excess water in each sample and the corresponding contribution from the ΔH°_f of water from the elements (see Table 5). The ΔH°_f values can be plotted as a function of water content (Fig. 3), and they fall on a line $\Delta H^{\circ}_f = -541.2 - 289.2x$, where x is the compositional variable in FeOOH•xH_2O. The slope of this line is close to the enthalpy of formation of liquid water from the elements, thus the water is loosely bound, most likely in significant proportion as water adsorbed on the surfaces or filling spaces between the particles. However, fitting a straight line through the acquired data eliminates the variation among the samples with differing crystallinity because the variation due to the large ΔH°_f of H_2O swamps the small effects of differences in crystallinity. To highlight the latter effect, instead of a single line, a set of lines can be generated, with

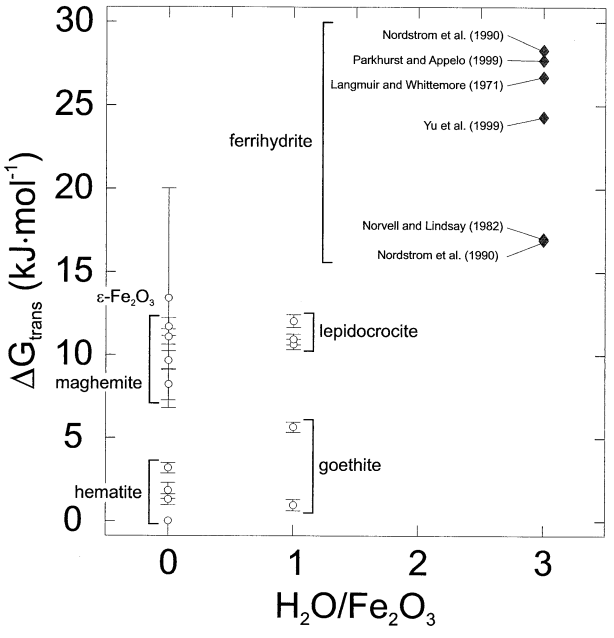

Fig. 1. Free energies of formation (ΔG_{trans}) of Fe(III) phases from $\frac{1}{2}\alpha$-Fe_2O_3 and liquid water. Data from: hematite (Robie and Hemingway, 1995), goethite, lepidocrocite, maghemite (Majzlan et al., 2003b). Multiple data points for hematite, goethite, lepidocrocite, and maghemite represent samples of those phases with variable surface areas (Majzlan, unpublished data). The data points for ferrihydrite were calculated from log K_8 or log K_9 (Table 1) and marked accordingly.

Table 2. Chemical analyses of lepidocrocite, ferrihydrite, and schwertmannite samples.

Sample	Weight loss after firing at 1200 K (%)	Fe/S (wt%/wt%)
Lepidocrocite	12.99[a] ± 0.14[b](12)[c]	n.a.[d]
fh0	16.79 ± 0.43(6)	n.a.
fh2	22.69 ± 0.29(5)	n.a.
fh6	19.78 ± 0.32(5)	n.a.
fh12	19.54 ± 0.45(9)	n.a.
fh24	18.70 ± 0.43(9)	n.a.
B1000S	31.21 ± 0.53(3)	11.12
Sch18	34.20 ± 0.27(4)	10.37

[a] Average.
[b] Two standard deviations of the mean.
[c] Number of experiments.
[d] Not applicable.

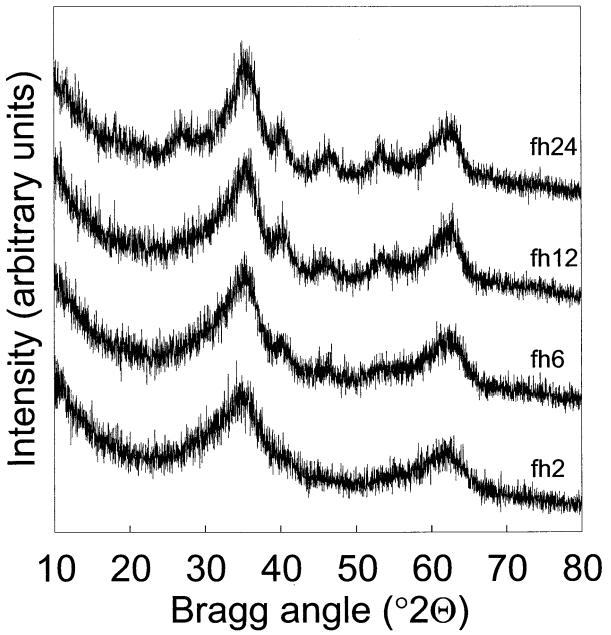

Fig. 2. X-ray diffraction patterns of ferrihydrite samples fh2 through fh24.

slopes fixed exactly at ΔH^o_f(water, l) (-285.8 ± 0.1 kJ•mol^{-1}). These lines allow one to obtain the enthalpy of formation of a chosen ferrihydrite composition by interpolation or extrapolation (Fig. 3). This ability to determine formation enthalpy of a chosen ferrihydrite composition is important because many previous studies disagree about the "nominal" composition of ferrihydrite, and the thermodynamic studies reviewed below considered ferrihydrite composition as $Fe(OH)_3$. The enthalpy of formation of $Fe(OH)_3$ 2-line ferrihydrite is -827.1 ± 2.0 kJ•mol^{-1}, and ΔH^o_f (6-line fh) is -830.3 ± 2.0 kJ•mol^{-1}.

The enthalpy of ferrihydrite relative to other iron oxides does not deviate strikingly from the transformation enthalpies among the other iron oxides (Fig. 4). The energetics of all iron oxides appears very closely balanced, except for goethite and hematite, two phases that define the energetic minima in the system.

The iron oxides are also closely balanced in terms of their free energies (Fig. 1). The standard entropies were measured for coarse-grained goethite, lepidocrocite, and maghemite (Majzlan et al., 2003a), and we neglect any small difference in standard entropies (S^o) between coarse- and fine-grained samples of the same phase. We also neglect any variation in S^o of maghemite because of vacancy ordering schemes; order or disorder of vacancies can modify S^o by a maximum of 2.0 J•mol^{-1}•K^{-1} (Majzlan et al., 2003a), corresponding to 0.6 kJ•mol^{-1} difference in ΔG at 298.15 K. This variation is not sufficient to alter the relations among maghemite and other iron oxide phases. The remaining data points in Figure 1 are free energies of transformation calculated from published equilibrium constants of reactions involving ferrihydrite. The estimates for equilibrium constants for reactions involving ferrihydrite of $Fe(OH)_3$ compositions are listed in Table 6. These estimates were reported for two reactions

Table 3. Enthalpies of solution (ΔH_{sol}) for the reference compounds, ferrihydrite and schwertmannite samples. Molar enthalpies given per mole of the formula listed in second column.

Sample	Formula	ΔH_{sol} (J · g^{-1})	ΔH_{sol} (kJ · mol^{-1})
Reference phases			
Lepidocrocite	$FeOOH \cdot 0.162H_2O$	-507.17[a] ± 2.56[b](6)[c]	$-46.54 \pm 0.23(6)$
Periclase	MgO	$-3713.9 \pm 21.9(6)$	$-149.69 \pm 0.88(6)$
α-$MgSO_4$	α-$MgSO_4$	$-430.68 \pm 8.25(6)$	$-51.84 \pm 0.99(6)$
Water	H_2O		-0.40[d]
Ferrihydrite			
fh0	$FeOOH \cdot 0.395H_2O$	$-571.90 \pm 4.68(6)$	$-54.88 \pm 0.45(6)$
fh2	$FeOOH \cdot 0.801H_2O$	$-513.56 \pm 8.31(8)$	$-53.04 \pm 0.86(8)$
fh6	$FeOOH \cdot 0.593H_2O$	$-531.85 \pm 4.25(5)$	$-52.94 \pm 0.42(5)$
fh12	$FeOOH \cdot 0.576H_2O$	$-533.10 \pm 3.27(5)$	$-52.90 \pm 0.32(5)$
fh24	$FeOOH \cdot 0.520H_2O$	$-526.31 \pm 3.44(5)$	$-51.70 \pm 0.34(5)$
Schwertmannite			
B1000S	$FeO(OH)_{0.686}(SO_4)_{0.157} \cdot 0.972H_2O$	$-322.27 \pm 4.98(6)$	$-37.41 \pm 0.58(6)$
Sch18	$FeO(OH)_{0.664}(SO_4)_{0.168} \cdot 1.226H_2O$	$-304.85 \pm 3.74(7)$	$-37.00 \pm 0.45(7)$

[a] Average.
[b] Two standard deviations of the mean.
[c] Number of experiments.
[d] Calculated from Parker (1965).

Table 4. Enthalpies of formation (ΔH_f^o) of the reference and studied compounds.

Sample	Formula	ΔH_f^o (kJ · mol^{-1})
Reference phases		
Lepidocrocite	γ-FeOOH	−549.4 ± 1.4[a]
Periclase	MgO	−601.6 ± 0.3[b]
α-$MgSO_4$	α-$MgSO_4$	−1288.8 ± 0.5[c]
Water	H_2O	−285.8 ± 0.1[b]
Ferrihydrite		
fh0	FeOOH · 0.395H_2O	−654.1 ± 1.2
fh2	FeOOH · 0.801H_2O	−772.1 ± 1.4
fh6	FeOOH · 0.593H_2O	−712.9 ± 1.2
fh12	FeOOH · 0.576H_2O	−708.1 ± 1.2
fh24	FeOOH · 0.520H_2O	−693.2 ± 1.2
Schwertmannite		
B1000S	$FeO(OH)_{0.686}(SO_4)_{0.157}$ · 0.972H_2O	−884.0 ± 1.3
Sch18	$FeO(OH)_{0.664}(SO_4)_{0.168}$ · 1.226H_2O	−960.7 ± 1.2

[a] Majzlan et al. (2003b).
[b] Robie and Hemingway (1995).
[c] Ko and Daut (1980), corrected by DeKock (1986).

$$Fe(OH)_3 + 3H^+ = Fe^{3+} + 3H_2O \quad (8)$$

$$Fe(OH)_3 = Fe^{3+} + 3OH^- \quad (9)$$

From each estimate, the Gibbs free energy of formation (ΔG_f^o) and Gibbs free energy with respect to hematite and liquid water (ΔG_{trans}) was calculated. Langmuir and Whittemore (1971) determined pK for reaction (9) listed in Table 6 as 37.3 to 43.3. The lowest pK value was measured for freshly precipitated amorphous material, the highest for aged, relatively well crystalline material consisting of goethite and lepidocrocite. Hence, the pK of 37.3 was used in the calculations as corresponding to 2-line ferrihydrite. Nordstrom et al. (1990) listed a range of log K instead of a single value.

The large spread of ΔG_{trans} of ferrihydrite (Fig. 1) is in sharp contrast with the balance of calculated ferrihydrite ΔH_{trans} (Fig. 4). We have two reasons to suspect that the estimates that give large ΔG_{trans} are problematic. First, in its dry form, ferrihydrite can persist for appreciable time, but free energies of large magnitude (30 kJ•mol^{-1}) indicate a large driving force for transformation, inconsistent with such persistence. Second, if we accept the small difference in enthalpies among ferrihydrite and the other iron oxides, the high ΔG_{trans} hint that ferrihydrite has an unusually low entropy, a possibility that is counterintuitive.

Table 5. Thermochemical cycle for acid solution calorimetry for ferrihydrite.

Reaction and reaction number	
γ-FeOOH · wH_2O (cr, 298 K) + [$3H^+$] (aq, 298 K) = [Fe^{3+} + (2+w)H_2O] (aq, 298 K)	2
FeOOH · xH_2O (s, 298 K) + [$3H^+$] (aq, 298 K) = [Fe^{3+} + (2+x)H_2O] (aq, 298 K)	3
H_2O (1, 298 K) = [H_2O] (aq, 298 K)	4
Fe (cr, 298 K) + O_2 (g, 298 K) + $\frac{1}{2}H_2$ (g, 298 K) = γ-FeOOH (cr, 298 K)	5
H_2 (g, 298 K) + $\frac{1}{2}O_2$ (g, 298 K) = H_2O (1, 298 K)	6
Fe (cr, 298 K) + (1 + x/2)O_2 (g, 298 K) + ($\frac{1}{2}$ + x)H_2 (g, 298 K) = FeOOH · xH_2O (s, 298 K)	7
$\Delta H_2 = \Delta H_{sol}$ (lepidocrocite)	
$\Delta H_3 = \Delta H_{sol}$ (ferrihydrite)	
$\Delta H_4 = \Delta H_{dilution}$	
$\Delta H_5 = \Delta H_f^o$ (lepidocrocite)	
$\Delta H_6 = \Delta H_f^o$ (water)	
$\Delta H_7 = \Delta H_f^o$ (ferrihydrite) = $\Delta H_2 - \Delta H_3 + (x - w)\Delta H_4 + \Delta H_5 + x\Delta H_6$	

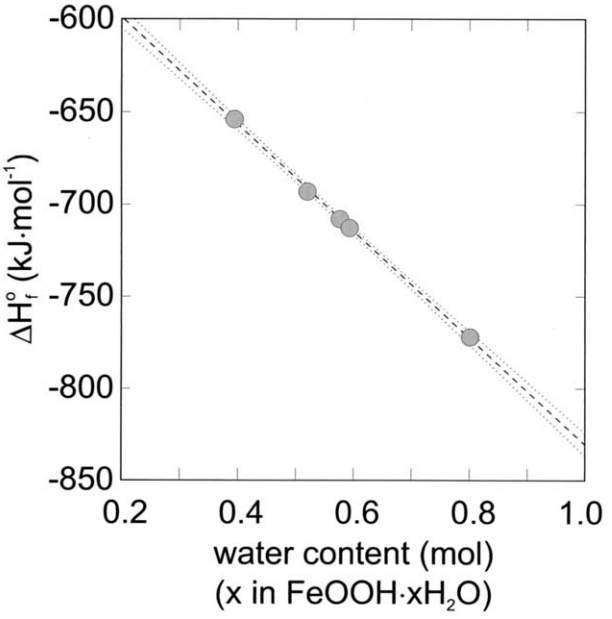

Fig. 3. Enthalpies of formation (ΔH^o_f) of ferrihydrite as a function of its water content. The error bars are smaller than the symbols. Only one line (the dashed line) fitting the data is shown, instead of a set of lines (discussed in text) because the set of lines would plot on the scale of this figure as a single line identical to the one drawn. The dotted curves mark 95% (2σ) confidence interval of the fit.

The standard entropy of ferrihydrite is not known but can be estimated. The entropy of reaction

$$\gamma\text{-FeOOH (cr,298 K)} + H_2O\ (1,298\ K) = Fe(OH)_3\ (\text{solid, 298 K}) \quad (10)$$

should be negative, because a solid and liquid water are reacting to form another solid. Hence, the standard entropy of ferrihydrite should be $<135.1\pm0.2$ J•mol^{-1}•K^{-1}.

The standard entropies of goethite, lepidocrocite, and maghemite (Majzlan et al., 2003a) correlate with the standard entropies of their isostructural Al counterparts (Fig. 5). Using a linear extrapolation, the entropy of a hypothetical gibbsite-like $Fe(OH)_3$ is 122.2 ± 0.6 J•mol^{-1}•K^{-1}. Because of significant disorder in ferrihydrite, the standard entropy of $Fe(OH)_3$ ferrihydrite should be larger than the S^o of any ordered, well-crystalline $Fe(OH)_3$, and therefore S^o (ferrihydrite) should be $>122.2\pm0.6$ J•mol^{-1}•K^{-1}.

Thus, the entropy of ferrihydrite could be constrained to lie between 122 and 135 J•mol^{-1}•K^{-1}. The free energies of formation in Table 6 can be combined with the extrapolated formation enthalpies to give the standard entropy of ferrihydrite and compared to the estimates above. Only one of the calcu-

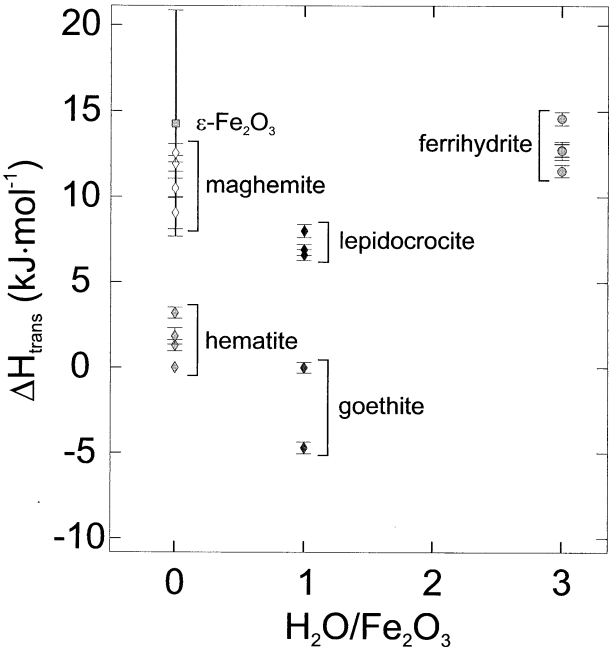

Fig. 4. Enthalpies of formation (ΔH_{trans}) of Fe(III) phases from $\frac{1}{2}\alpha$-Fe_2O_3 and liquid water. Data from: hematite (Robie and Hemingway, 1995), goethite, lepidocrocite, maghemite (Majzlan et al., 2003b), ferrihydrite (this study). Multiple data points for hematite, goethite, lepidocrocite, and maghemite represent samples of those phases with variable surface areas (Majzlan, unpublished data).

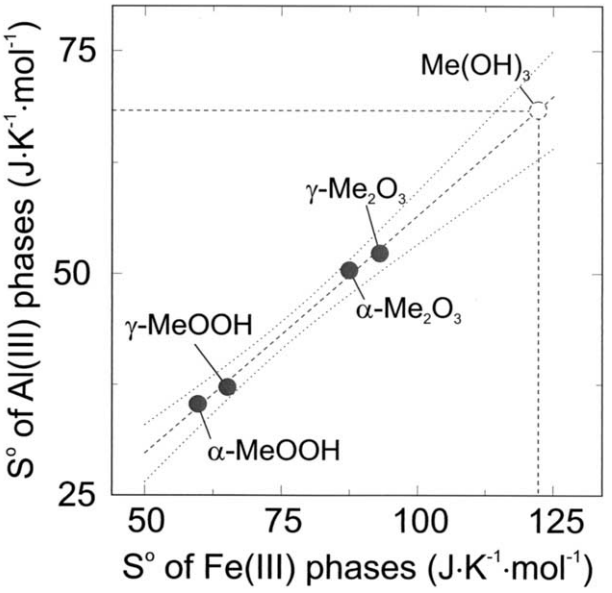

Fig. 5. Standard entropies of pairs of isostructural Fe(III) and Al(III) phases: hematite — corundum, diaspore — goethite, boehmite — lepidocrocite, γ-Al_2O_3 — maghemite, gibbsite — $Fe(OH)_3$ (data from Robie and Hemingway, 1995; Chase, 1998; Majzlan et al., 2003a). Solid symbols: values known for both Fe(III) and Al(III) compounds; open symbol: extrapolation for $Fe(OH)_3$ based on the known value for gibbsite. The dotted curves mark 95% (2σ) confidence interval of the fit.

lated S^o values fall within the entropy range predicted, and the lower entropy values that correspond to less exothermic ΔG^o_f are furthest from the estimates. From the S^o values in Table 6, it appears that the entropy of reaction (10) may be positive, suggesting that the disorder in ferrihydrite is sufficient to offset the entropy loss due to locking liquid water in a solid. If the entropy of (10) is positive, one may argue that at a certain elevated temperature, ferrihydrite will become the stable phase. This stability reversal is unlikely because (1) the ΔH_{10} is sufficient to prevent ferrihydrite from being stable over a range of several 100 K (the exact range depends on the choice of ΔS_{10}) above 298 K, and (2) above 373 K, water will vaporize and the entropy of steam will completely swamp any entropy variations dictated by the solids; in reaction (10), the less hydrated phase (lepidocrocite) will be favored. In short, ferrihydrite cannot be concluded to become stable at any P-T.

Table 6. Available thermodynamic data for ferrihydrite. The standard entropies were calculated using the ΔH^o_f for 2-line ferrihydrite (-827.1 ± 2.0 kJ · mol^{-1}).

Reported quantity	Calculated ΔG^o_f (kJ · mol^{-1}); S^o (J · mol^{-1} · K^{-1})	Reference
log K_8 = 4.891	−700.2; 105.2	Truesdell and Jones (1974)
log K_8 = 3.0 to 5.0	−711.0 to −699.6; 141.4 to 103.2	Nordstrom et al. (1990)
log K_8 = 4.3 ± 0.5	−703.6 ± 3.5; 116.6	Yu et al. (1999)
log K_8 = 3.55 ± 0.1	−707.9 ± 2.1; 131.0	Schindler et al. (1963)
pK_9 = 37.3 to 43.3	−701.2; 108.6 for pK_9 = 37.3[a]	Langmuir and Whittemore (1971)
log K_9 = −39	−710.9; 141.1	Norvell and Lindsay (1982)

[a] See text.

We selected the "best" set of thermodynamic data for ferrihydrite of composition $Fe(OH)_3$, following the discussion above, according to two requirements. First, ferrihydrite is required to be metastable with respect to lepidocrocite, which is a reasonable assumption since ferrihydrite has been observed to convert spontaneously to lepidocrocite (Langmuir and Whittemore, 1971). Hence, the lower bound on ΔG^o_f of ferrihydrite is -715.5 ± 2.0 kJ•mol^{-1}, and the lower limit of log K_8 is 2.21 ± 0.50. The lower bound on ΔG^o_f and log K_8 was calculated using thermodynamic data for a lepidocrocite sample with surface area of 80 m^2/g ($\Delta H^o_f = -548.0 \pm 1.3$ kJ•mol^{-1}; Majzlan, unpublished data). Second, the standard entropy of ferrihydrite is required to be $>122.2 \pm 0.6$ J•mol^{-1}•K^{-1}, based on the extrapolation shown in Figure 5. This requirements sets the upper limit for log K_8 (2-line ferrihydrite) at 4.01 ± 0.50, and the upper limit for log K_8 (6-line ferrihydrite) at 3.44 ± 0.50.

The lower limit for ΔG^o_f and log K_8, set by the requirement of metastability of ferrihydrite to lepidocrocite, leads to a rather low log $K_8 = 2.21 \pm 0.50$. None of the published log K_8 estimates is as low as our lower bound, and the range given by Nordstrom et al. (1990) extends only from 3.0 to 5.0. The lower bound on ΔG^o_f of ferrihydrite sets this compound in equilibrium with fine-grained lepidocrocite and liquid water. The low log K_8 value suggests that such equilibrium should not

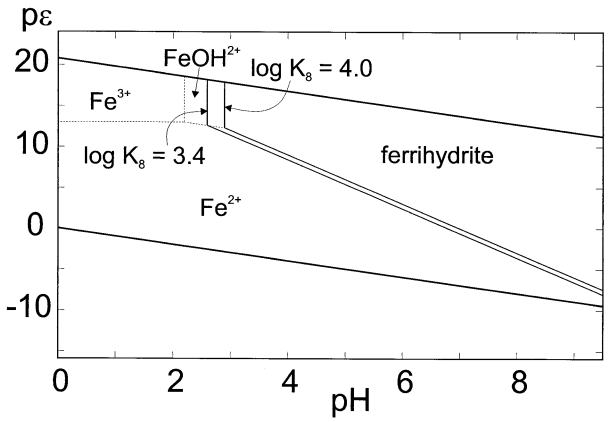

Fig. 6. pH-pε diagram for the estimated log K_8 range for 2-line ferrihydrite, assuming activity of 10^{-4} for dissolved iron. Stability field of ferrihydrite shown for both lower and upper limit of log K_8 (Table 1). Equilibrium constants for aqueous species from Nordstrom and Munoz (1994).

be considered as realistic, and the lower bound should be set higher. Summarizing, the log K_8 for 6-line ferrihydrite is 3.0 ± 0.5–3.4 ± 0.5. 2-line ferrihydrite is less stable than 6-line ferrihydrite, and so log K_8 for 2-line ferrihydrite is best described by a range of 3.4 ± 0.5–4.0 ± 0.5. Calculated per mole of $Fe(OH)_3$, 2-line and 6-line ferrihydrite are 19.4 ± 2.1–22.7 ± 2.1 and 16.9 ± 2.1–19.4 ± 2.1 kJ•mol^{-1} metastable with respect to hematite and liquid water, respectively. The selected thermodynamic data for ferrihydrite are summarized in Table 1. From these data, 2-line ferrihydrite can be shown to precipitate from water with $a(Fe^{3+}) = 10^{-4}$ at pH = 2.6–2.9 (Fig. 6).

3.3. Schwertmannite

Chemical compositions and enthalpies of solution of schwertmannite samples and reference compounds are given in Tables 2 and 3. XRD pattern of the sample B1000S is given in Bigham et al. (1990, their Fig. 3), and the pattern of Sch18 is similar to that of B1000S. The pattern consists of six distinct broad maxima and several shoulders, all indexed on the basis of akaganeite unit cell. Bigham et al. (1990) also showed the IR spectra of synthetic schwertmannite samples, locating and assigning ν_3, ν_1, and ν_4 bands of the sulfate group, OH stretching and bending mode, and H_2O deformation mode. Their Mössbauer spectroscopy results suggests average magnetic ordering temperature of 75 K.

Table 8. Available thermodynamic data for schwertmannite. The quantity q describes chemical composition of schwertmannite in $FeO(OH)_{1-2q}(SO_4)_q$.

q	Reported quantity	Reference
0.131	$\log K_{21} = 0.88 \pm 0.01$	Kawano and Tomita (2001)
0.225	$\log K_{21} = 1.31 \pm 0.31$	Yu et al. (1999)
0.200	$\log K_{21} = 2.25 \pm 0.31$	Bigham et al. (1996)

Because schwertmannite contains sulfate anion, additional reference compounds, periclase (MgO) and α-$MgSO_4$, had to be used in the thermochemical cycle (Table 7).

The thermodynamic data for ferrihydrite can be combined with the published data for schwertmannite (Table 8) to construct pε-pH diagrams for these two minerals and pyrite (FeS_2) (Fig. 7). The lower limit of schwertmannite stability was calculated from

$$FeO(OH)_{1-2q}(SO_4)_q + (3-2q)H^+ = Fe^{3+} + qSO_4^{=} + (2-2q)H_2O \quad (21)$$

$$pH_{21} = (-\log \alpha(Fe^{3+}) - q\log a(SO_4^{=}) + \log K_{21})/(3-2q)$$

$$FeO(OH)_{1-2q}(SO_4)_q + (2-2q)H^+ = FeOH^{2+} + qSO_4^{=} + (1-2q)H_2O \quad (22)$$

$$pH_{22} = (-\log a(FeOH^{2+}) - q\log a(SO_4^{=}) + \log K_{22})/(2-2q),$$

for the predominance field of Fe^{3+} and $FeOH^{2+}$, respectively.

Table 7. Thermochemical cycle for acid solution calorimetry for schwertmannite.

Reaction and reaction number	
H_2O (1,298 K) = [H_2O] (aq,298 K)	11
γ-FeOOH · wH_2O (cr,298 K) + 3 [H^+] (aq,298 K) = [Fe^{3+}] (aq,298 K) + (2+w)[H_2O] (aq,298 K)	12
α-$MgSO_4$ (cr,298 K) = [Mg^{2+}] (aq,298 K) + [$SO_4^{=}$] (aq,298 K)	13
MgO (cr,298 K) + 2[H^+] (aq,298 K) = [Mg^{2+}] (aq,298 K) + [H_2O] (aq,298 K)	14
$FeO(OH)_{1-2q}(SO_4)_q$ · sH_2O (s,298 K) + (3−2q)[H^+] (aq,298 K) = [Fe^{3+}] (aq,298 K) + q[$SO_4^{=}$] (aq,298 K) + (2−2q+s)[H_2O] (aq,298 K)	15
Fe (cr,298 K) + O_2 (g,298 K) + 1/2H_2 (g,298 K) = γ-FeOOH (cr,298 K)	16
Mg (cr,298 K) + S (cr,298 K) + 2O_2 (g,298 K) = α-$MgSO_4$ (cr,298 K)	17
Mg (cr,298 K) + 1/2O_2 (g,298 K) = MgO (cr,298 K)	18
H_2 (g,298 K) + 1/2O_2 (g,298 K) = H_2O (1,298 K)	19
Fe (cr,298 K) + qS (cr,298 K) + (1+q+s/2)O_2 (g,298 K) + (1/2 −q+s)H_2 (g,298 K) = $FeO(OH)_{1-2q}(SO_4)_q$ · sH_2O (s,298 K)	20
$\Delta H_{11} = \Delta H_{dilution}$	
$\Delta H_{12} = \Delta H_{sol}$ (lepidocrocite)	
$\Delta H_{13} = \Delta H_{sol}$ (α-$MgSO_4$)	
$\Delta H_{14} = \Delta H_{sol}$ (periclase)	
$\Delta H_{15} = \Delta H_{sol}$ (schwertmannite)	
$\Delta H_{16} = \Delta H_f^o$ (lepidocrocite)	
$\Delta H_{17} = \Delta H_f^o$ (α-$MgSO_4$)	
$\Delta H_{18} = \Delta H_f^o$ (periclase)	
$\Delta H_{19} = \Delta H_f^o$ (water)	
$\Delta H_{20} = \Delta H_f^o$ (schwertmannite) = (s-q-w)ΔH_{11} + ΔH_{12} + qΔH_{13} − qΔH_{14} − ΔH_{15} + ΔH_{16} + qΔH_{17} − qΔH_{18} + (s-q)ΔH_{19}	

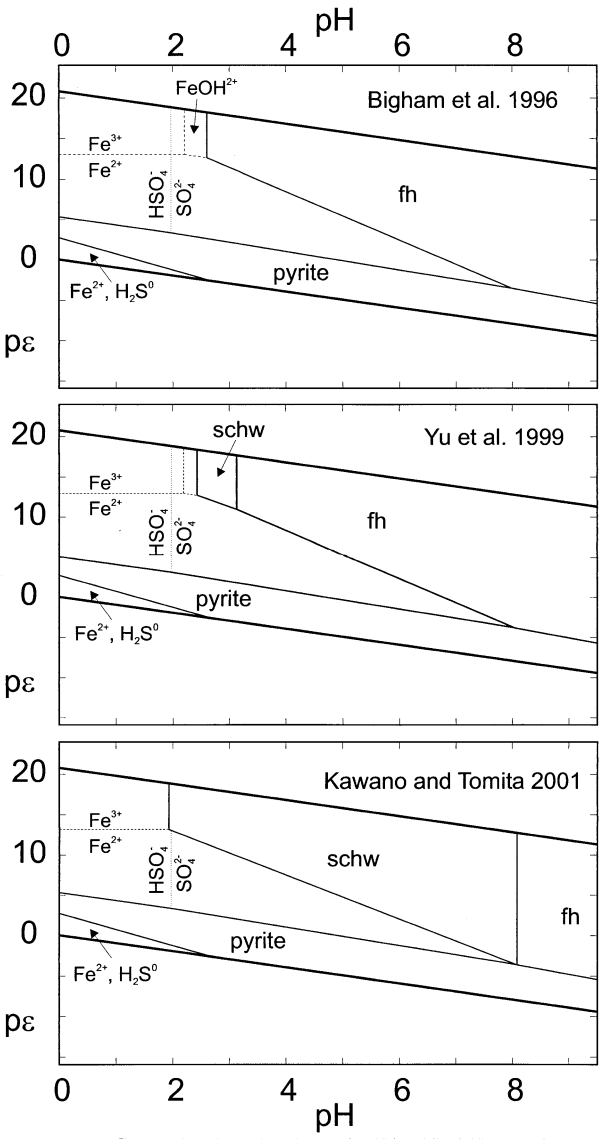

Fig. 7. pH-pε diagrams with three published estimates of log K_{21} (Table 8) for schwertmannite, assuming activities of 10^{-4} for dissolved iron and 10^{-3} for dissolved sulfur. Equilibrium constants for aqueous species from Nordstrom and Munoz (1994). Thermodynamic data for pyrite from Robie and Hemingway (1995).

The pH at which schwertmannite and ferrihydrite coexist was calculated from

$$FeO(OH)_{1-2q}(SO_4)_q + (1 + 2q)H_2O = Fe(OH)_3 + qSO_4^{=} + 2qH^+ \quad (23)$$

$$pH_{23} = (q\log a(SO_4^{=}) - \log K_{21} + \log K_8)/2q.$$

The activities of the aqueous species in Figures 6–9 were fixed at 10^{-4} for dissolved iron and 10^{-3} for dissolved sulfur. These values are close to the concentration of ferric iron and sulfate ion encountered in the work on solubility of natural schwertmannite (Yu et al., 1999; Kawano and Tomita, 2001). The solubility product of ferrihydrite (log K_8) was taken as 3.4.

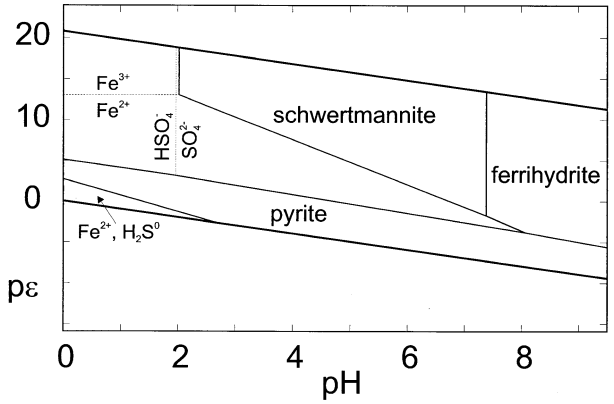

Fig. 8. pH-pε diagram for ferrihydrite and schwertmannite, drawn using the equilibrium constants estimated in this work (log K_8 = 3.4, Table 1). See captions for Figure 7 for further details.

While the schwertmannite stability field does not appear when the K_{sp} of Bigham et al. (1996) is used (Fig. 7), the K_{sp} of Kawano and Tomita (2001) gives schwertmannite a stability field covering acidic, neutral, and mildly alkaline waters. We must stress that the diagrams in Figure 7 are only an illustration of relations between the solids whose stability fields are plotted. These diagrams are *not* used to constrain any thermodynamic quantity reported in this work. Instead, the diagrams in Figure 7 (as well as Figs. 8 and 9) are calculated from the thermodynamic data found in cited references or derived as described in the text.

As in the case of ferrihydrite, the standard entropy of schwertmannite is not known but can be approximated. The standard entropies of polymorphs in general increase with increasing molar volumes (Holland, 1989). The molar volumes of goethite, lepidocrocite, akaganeite, and schwertmannite are 20.9, 22.4, 25.5, and 25.8 cm^3, respectively (Bigham et al., 1990; Post and Buchwald, 1991; Majzlan et al., 2003a). The entropy of goethite is 59.7±0.2 J•mol^{-1}•K^{-1}, and that of lepidocrocite is 65.1±0.2 J•mol^{-1}•K^{-1} (Majzlan et al., 2003a). The entropy

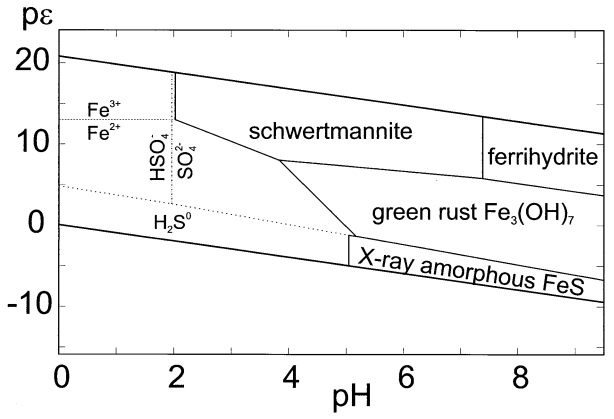

Fig. 9. pH-pε diagram for poorly crystalline iron oxides and sulfides, assuming activities of 10^{-4} for dissolved iron and 10^{-3} for dissolved sulfur. Equilibrium constants for aqueous species from Nordstrom and Munoz (1994). Thermodynamic data for green rust from Bourrié et al. (1999), for X-ray amorphous FeS from Truesdell and Jones (1974).

of a tunnel FeOOH framework is then 76.3±0.8 J•mol^{-1}•K^{-1} for akaganeite and 77.3±0.8 J•mol^{-1}•K^{-1} for a hypothetical ordered schwertmannite framework. Three additional contributions to the entropy of schwertmannite have to be considered. The first is the entropy due to hydroxyl-sulfate substitution. The second is the entropy of excess water; this entropy likely lies between the entropy of hexagonal ice (41.3±0.1 J•mol^{-1}•K^{-1}, Debye-Einstein fitting and extrapolation of data in Giauque and Stout, 1936, see Majzlan et al., 2003a) and the entropy of liquid water (70.0±0.1 J•mol^{-1}•K^{-1}, Robie and Hemingway, 1995). The third contribution arises from disorder in the compound. None of these contributions is constrained well enough to provide a reasonable estimate of S^o(schwertmannite). The lower limit for the entropies of the studied samples consists of 77.3 J•mol^{-1}•K^{-1} for the framework, 41.3 J•mol^{-1}•K^{-1} for each mole of excess water, and an assumed 10% increase of the sum of these two contributions due to sulfate-hydroxyl substitution, disorder, and excess water entropy. The 10% increase is arbitrary, and therefore the entropy estimate is uncertain, but sufficient to demonstrate the point made in the following paragraph.

The measured enthalpy of formation and estimated entropy are combined into the Gibbs free energy of formation (ΔG^o_f) of schwertmannite, giving $\Delta G^o_f = -761.3 \pm 1.3$ kJ•mol^{-1} for $FeO(OH)_{0.686}(SO_4)_{0.157}$•$0.972H_2O$ and $\Delta G^o_f = -823.3 \pm 1.2$ kJ•mol^{-1} for $FeO(OH)_{0.664}(SO_4)_{0.168}$•$1.226H_2O$. The corresponding solubility product is then used to calculate the stability field of schwertmannite with respect to ferrihydrite (Fig. 8). Realizing again that we used a lower limit for S^o(schwertmannite) in these calculations, increasing this entropy will further enlarge the stability field of schwertmannite. Therefore, the thermodynamic data collected in this study suggest that schwertmannite is thermodynamically favored over ferrihydrite over a wide range of pH when the system contains even a small amount of sulfate. The thermodynamic stability of schwertmannite over ferrihydrite is probably the result of the better crystallinity of the former. Moreover, further stabilization of the surface of schwertmannite particle may be achieved by adsorption of the sulfate groups. Given that both ferrihydrite and schwertmannite typically have large specific surface area, any stabilization of the exposed surfaces may lead to significant stabilization of the compound.

The stability relations of the two investigated samples can be replicated by that of schwertmannite of the "ideal" composition $FeO(OH)_{3/4}(SO_4)_{1/8}$ with $\Delta G^o_f = -518.0 \pm 2.0$ kJ•mol^{-1}. This value and the corresponding stability field are closest to those proposed by Kawano and Tomita (2001). The other thermodynamic values for schwertmannite (Bigham et al., 1996; Yu et al., 1999) probably represent either variation in the natural material or a value modified by interference of other ions or organic matter in the natural samples.

3.4. Application to natural systems

Many thermodynamic studies are performed with an implicit assumption that their results are applicable to a more complex system of similar chemical composition and internal structure. The thermodynamic investigations are often performed on a well defined single phase or mixture of phases. A phase is defined (Gibbs, 1875) as a homogeneous body that can be formed out of any set of component substances, where the term homogeneous implies both uniform chemical composition and physical state. Coexisting phases are then separated by dividing surfaces. Some of the poorly crystalline iron oxides may not fit this strict definition, and the implicit assumption of transferability of the thermodynamic results may be invalid. In particular, Janney et al. (2000a) found that the ferrihydrite sample available to them was a mixture of nanocrystallites with several distinct structures and disordered variants thereof, violating the requirement of chemical and physical homogeneity. Moreover, 6-line fh is not simply a more crystalline version of the 2-line fh (Janney et al., 2000a), thus violating an assumption of uniformity of this compound with varying crystallinity. The separation of coexisting phases by well defined dividing surfaces implies that such phases should be separable by mechanical means. Ferrihydrite is mechanically separable from suspension in water. However, dried ferrihydrite may not correspond in various properties to the parent ferrihydrite suspension, implying that the mechanical separation and drying may alter the substance. For example, Shinoda et al. (1994) found that the coordination of iron in ferrihydrite suspension and freeze-dried ferrihydrite is mostly octahedral, but the way the octahedra link to each other is different for the two cases.

The question of applicability of the results arises especially in the case of ferrihydrite. For schwertmannite and ε-Fe_2O_3, at least a few relatively well defined Bragg diffraction peaks allow appropriate recognition and structural characterization, and we consider the presented results transferable to other samples. In the case of ferrihydrite, we suggest only a range of possible free energies and equilibrium constants, supported by the experimentally measured formation enthalpies, estimates of standard entropy, and log K estimates from natural systems. Following the discussion above, any log K_8 outside the range given in this work would imply either unusually low entropy or stability of ferrihydrite with respect to one of the well-crystalline iron oxide phases. The ranges given (Table 1) are perhaps wider than desired for geochemical modeling of natural systems, but the widths of these ranges document both the difficulties in experimental study of poorly crystalline and poorly known compounds and the intrinsic variability of ferrihydrite in natural settings. The new data place tighter constraints on the properties of this complex set of compounds than the earlier studies. Further uncertainties in the studies on natural ferrihydrite samples arise from substitution of other metals (Al, Mn) for iron, adsorption of ions (SO_4^{2-}, AsO_4^{3-}) or neutral molecules (CO_2), incorporation of organic matter, and aggregation of ferrihydrite as a response to wetting and drying. All these processes may modify the thermodynamics of ferrihydrite and were not considered in the present study. We recognize their importance, however, in this study we focused on chemically pure, dry ferrihydrite only.

4. CONCLUSIONS

We present new data for free energies and solubility products of ferrihydrite, schwertmannite, and ε-Fe_2O_3 based on enthalpies of formation measured under controlled conditions on well characterized samples. Additional constraints on the thermodynamic data came from estimates of entropy, published estimates of solubility products of these phases, and observations in natural systems. The data collected in this study can be

combined with thermodynamic data for other poorly crystalline iron compounds to draw a more complete phase diagrams (Fig. 9). This diagram illustrates the thermodynamic relationships in the initial stages of iron precipitation from aqueous solutions, in acid mine drainage waters (precipitating ferrihydrite and schwertmannite), redoximorphic soils (green rust), or reduced marine sediments such as those in Black Sea (amorphous iron sulfides). At the same time, this diagram does not capture the effect of kinetic factors on the precipitation and ageing process. The interplay between thermodynamics and kinetics should be always born in mind, especially because disequilibrium in these systems is common. We are working on thermodynamics of well-crystalline iron sulfate minerals (e.g., rhomboclase, copiapite) to complete the thermodynamic description of iron and sulfate precipitation in relatively oxidized systems, such as acid waste waters, from the initial to late stages.

Acknowledgments—We thank P. Buseck, D. Sherman, D. Wesolowski, and two anonymous reviewers for valuable comments that improved the quality of the manuscript. This study was financially supported by the Department of Energy, grant DE-FG0301ER 15237.

Associate editor: D. Wesolowski

REFERENCES

Bigham J. M., Schwertmann U., Carlson L., and Murad E. (1990) A poorly crystallized oxyhydroxysulfate of iron formed by bacterial oxidation of Fe(II) in acid mine waters. *Geochim. Cosmochim. Acta* **54,** 2743–2758.

Bigham J. M., Schwertmann U., Traina R. L., Winland R. L., and Wolf M. (1996) Schwertmannite and the chemical modeling of iron in acid sulfate waters. *Geochim. Cosmochim. Acta* **60,** 2111–2121.

Bourrié G., Trolard F., Génin J.-M. R., Jaffrezic A., Maître V., and Abdelmoula M. (1999) Iron control by equilibria between hydroxy-Green Rusts and solutions in hydromorphic soils. *Geochim. Cosmochim. Acta* **63,** 3417–3427.

Chase M. W. Jr. (1998) NIST-JANAF thermochemical tables. Fourth edition. *J. Phys. Chem. Ref. Data*, monograph no. **9**.

Clausen L. and Fabricius I. (2001) Atrazine, isoproturon, mecoprop, 2,4-D, and bentazone adsorption onto iron oxides. *J. Environ. Qual.* **30,** 858–869.

DeKock C. W. (1986) Thermodynamic properties of selected metal sulfates and their hydrates. *Bur. Mines, Inf. Circ.* 9081.

Drits V. A., Sakharov B. A., Salyn A. L., and Manceau A. (1993) Structural model for ferrihydrite. *Clay Miner.* **28,** 185–207.

Giauque W. F. and Stout J. W. (1936) The entropy of water and the third law of thermodynamics. The heat capacity of ice from 15 to 273°K. *J. Am. Chem. Soc.* **58,** 1144–1150.

Gibbs J. W. (1875) On the equilibrium of heterogeneous substances. *Trans. Conn. Acad., III.*, 108–248:Reprinted in: (1993) The Scientific Papers of J. Willard Gibbs, Ph.D., LL.D. Volume I: Thermodynamics. pp. 55–371. Ox Bow Press, Woodbridge, Connecticut.

Holland T. J. B. (1989) Dependence of entropy on volume for silicate and oxide minerals: A review and a predictive model. *Am. Miner.* **74,** 5–13.

Jambor J. L. and Dutrizac J. E. (1998) Occurrence and constitution of natural and synthetic ferrihydrite, a widespread iron oxyhydroxide. *Chem. Rev.* **98,** 2549–2585.

Janney D. E., Cowley J. M., and Buseck P. R. (2000a) Structure of synthetic 2-line ferrihydrite by electron nanodiffraction. *Am. Miner.* **85,** 1180–1187.

Janney D. E., Cowley J. M., and Buseck P. R. (2000b) Transmission electron microscopy of synthetic 2- and 6-line ferrihydrite. *Clays Clay Miner.* **48,** 111–119.

Janney D. E., Cowley J. M., and Buseck P. R. (2001) Structure of synthetic 6-line ferrihydrite by electron nanodiffraction. *Am. Miner.* **86,** 327–335.

Jansen E., Kyek A., Schafer W., and Schwertmann U. (2002) The structure of six-line ferrihydrite. *Appl. Phys. A.* **74**(supplement S)**,** S1004–S1006.

Kawano M. and Tomita K. (2001) Geochemical modeling of bacterially induced mineralization of schwertmannite and jarosite in sulfuric acid spring water. *Am. Miner.* **86,** 1156–1165.

Ko H. C. and Daut G. E. (1980) Enthalpies of formation of α- and β-magnesium sulfate and magnesium sulfate monohydrate. *Bur. Mines, Rep. Invest.* 8409.

Laberty C. and Navrotsky A. (1998) Energetics of stable and metastable low-temperature iron oxides and oxyhydroxides. *Geochim. Cosmochim. Acta* **62,** 2905–2913.

Lagmuir D. and Whittemore D. O. (1971) Variations in the stability of precipitated ferric oxyhydroxides. In *Nonequilibrium systems in natural water chemistry* (ed. J.D. Hem), pp. 209–234. American Chemical Society (*Advanced Chemistry Series* **106**).

Leone P., Negre M., Gennari M., Boero V., Celis R., and Cornejo J. (2002) Adsorption of imidazolinone herbicides on smectite-humic acid and smectite-ferrihydrite associations. *J. Agr. Food Chem.* **50,** 291–298.

Majzlan J., Lang B. E., Stevens R., Navrotsky A., Woodfield B. F., and Boerio-Goates J. (2003a) Thermodynamics of iron oxides. I. Standard entropy and heat capacity of goethite (α-FeOOH), lepidocrocite (γ-FeOOH), and maghemite (γ-Fe_2O_3). *Am. Miner.* **88,** 846–854.

Majzlan J., Grevel K.-D., and Navrotsky A. (2003b) Thermodynamics of iron oxides. II. Enthalpies of formation and relative stability of goethite (α-FeOOH), lepidocrocite (γ-FeOOH), and maghemite (γ-Fe_2O_3). *Am. Miner.* **88,** 855–859.

Manceau A. and Drits V. A. (1993) Local structure of ferrihydrite and feroxyhyte by EXAFS spectroscopy. *Clay Miner.* **28,** 165–184.

McClean R. G., Schofield M. A., Kean W. F., Sommer C. V., Robertson D. P., Toth D., and Gajdardzinska-Josifovska M. (2001) Botanical iron minerals: correlation between nanocrystal structure and modes of biological self-assembly. *Eur. J. Miner.* **13,** 1235–1242.

Nordstrom D. K. and Munoz J. L. (1994) Geochemical Thermodynamics. Blackwell Scientific Publications, 493 pp.

Nordstrom D. K., Plummer L. N., M Langmuir D., Busenberg E., May H. M., Jones B. F. and Parkhurst D. L. (1990) Revised chemical equilibrium data for major water-mineral reactions and their limitations. In *Chemical modeling in aqueous systems II* (ed. D.D. Melchior and R.L. Bassett), pp. 398–413. American Chemistry Society (*Symposium Series* **416**).

Norvell W. A. and Lindsay W. L. (1982) Estimation of the concentration of Fe^{3+} and the $(Fe^{3+})(OH^-)$ ion product from equilibria of EDTA in soil. *J. Soil Sci. Soc. Am.* **46,** 710–715.

Parker V. B. (1965) Thermal properties of uni-univalent electrolytes. *Natl. Stand. Ref. Data Ser., NBS* **2,** 66 pp.

Post J. E. and Buchwald V. F. (1991) Crystal structure refinement of akaganeite. *Am. Miner.* **76,** 272–277.

Robie R. A. and Hemingway B. S. (1995) Thermodynamic properties of minerals and related substances at 298.15 K and 1 bar (10^5 pascals) and at higher temperatures. *U.S. Geol. Survey Bull.* **2131,** 461 pp.

Scheinost A. C., Abend S., Pandya K. I., and Sparks D. L. (2001) Kinetic controls on Cu and Pb sorption by ferrihydrite. *Environ. Sci. Technol.* **35,** 1090–1096.

Schindler P., Michaelis W., and Feitknecht W. (1963) Die Löslichkeit gealterte Eisen(III)-hydroxid-Fällungen. *Helv. Chim. Acta* **46,** 444–449.

Schwertmann U. and Cornell R. M. (2000) Iron oxides in the laboratory. 2nd edition, Wiley-VCH, 188 pp.

Shinoda K., Matsubara E., Muramatsu A., and Waseda Y. (1994) Local structure of ferric hydroxide $Fe(OH)_3$ in aqueous solution by the anomalous X-ray scattering and EXAFS methods. *Mater. Trans., JIM.* **35,** 394–398.

Taylor J. R. (1982) An Introduction to Error Analysis. The Study of Uncertainties in Physical Measurements. University Science Books, 270 pp.

Trautmann J.-M. (1966) Détermination des enthalpies de formation standard des oxydes γ et εFe_2O_3. *Bull. Soc. Chim. Franc.* **3,** 992–994.

Tronc E., Chaneac C., and Jolivet J. P. (1998) Structural and magnetic characterization of ε-Fe_2O_3. *J. Solid State Chem.* **139,** 93–104.

Truesdell A. H. and Jones B. F. (1974) WATEQ, a computer program for calculating chemical equilibria of natural waters. *J. Res. U. S. Geol. Survey* **2,** 233–246.

Waychunas G. A, Myneni S. C. B, Traina S. J, Bigham J. M, Fuller C. C, and Davis J. A (2001) Reanalysis of the schwertmannite structure and the incorporation of SO_4^{2-} groups: An IR, XAS, WAXS and simulation study. *Abstracts of the 11th Goldschmidt conference*.

Yu J.-Y., Heo B., Choi I.-K., Cho J.-P., and Chang H.-W. (1999) Apparent solubilities of schwertmannite and ferrihydrite in natural stream waters polluted by mine drainage. *Geochim. Cosmochim. Acta* **63,** 3407–3416.